Elastic scattering calculations for electrons and positrons in solid targets

Maurizio Dapor

Citation: J. Appl. Phys. **79**, 8406 (1996); doi: 10.1063/1.362514
View online: http://dx.doi.org/10.1063/1.362514
View Table of Contents: http://jap.aip.org/resource/1/JAPIAU/v79/i11
Published by the American Institute of Physics.

Elastic scattering calculations for electrons and positrons in solid targets

Maurizio Dapor
Istituto Trentino di Cultura, I-38050 Povo, Trento, Italy

(Received 6 October 1995; accepted for publication 31 January 1996)

The differential, total, and transport cross sections for electrons and positrons impinging on free atoms and solid targets have been calculated in the energy range of 100–5000 eV. As an application, the mean number of the wide angle collisions suffered by the particle before slowing down to rest and the backscattering coefficient are analytically calculated; The values of backscattering coefficients are found to be in better agreement with experiment than earlier calculations. © *1996 American Institute of Physics.* [S0021-8979(96)04711-1]

I. INTRODUCTION

The transport of low energy electrons and positrons in solid targets is of great importance in electron spectroscopy and microscopy, electron microlithography, and positron annihilation spectroscopy.[1–5]

Both the Monte Carlo simulations and the analytical methods require an accurate knowledge of the elastic scattering cross sections. Unfortunately the differential elastic scattering cross section of charged particles interacting with free and bound atoms, particularly for low–medium kinetic energies, is not computable by using simple closed formulas.

The elastic scattering process can be described by calculating the phase shifts. Since the large-r asymptotic behavior of the radial wave function is known, the phase shifts can be computed by numerically solving the Dirac equation for a central electrostatic field up to a large radius where the atomic potential is negligible (typically 2 Å).

When the atom is bound in a solid the potential for interaction between the charged particle and the atom is different from the charged particle–free atom interaction potential due to the crystalline structure. In this article, differential, total, and transport cross sections for electrons and positrons will be calculated considering the solid state effects. The energy range of interest will be 100–5000 eV.

In order to discuss an important application, the computation of the mean number of wide-angle collisions suffered by the particle before slowing down to rest will be considered. Such a quantity is related to the so-called reflection coefficient. By using the present transport model in the examined energy range ($E<5$ keV) it will be shown that the mean number of wide-angle collisions before rest is always smaller for positrons than for electrons. Since the electrons suffer wide-angle collisions more frequently than positrons do before slowing down to rest, it can be concluded that electrons have a larger probability of backscattering than positrons. This conclusion is in accordance with recent reliable experimental data.

II. THEORETICAL REMARKS

As shown by Lin, Sherman, and Percus[6] and by Bunyan and Schonfelder,[7] the Dirac equation can be reduced to the following first-order differential equation:

$$\frac{d\phi_l^{\pm}(r)}{dr}=\frac{k^{\pm}}{r}\sin[2\phi_l^{\pm}(r)]-\cos[2\phi_l^{\pm}(r)]+W-V(r), \tag{1}$$

where the function $\phi_l^{\pm}(r)$ is related to the phase shifts, W is the total energy expressed in units of mc^2, and the lengths r are expressed in $h/(2\pi mc)$ (m=electron mass, c=speed of light, h=Planck's constant). The $^{\pm}$ symbols denote the spin-up and the spin-down cases: in particular $k^{+}=-l-1$ (and $j=l+1/2$) while $k^{-}=l$ (and $j=l-1/2$). For each quantum number l, the two phase shifts $\delta_l^{\pm}$ can be obtained by using

$$\tan\delta_l^{\pm}=\frac{Kj_{l+1}(Kr)-j_l(Kr)[(W+1)\tan\phi_l^{\pm}+(1+l+k^{\pm})/r]}{Kn_{l+1}(Kr)-n_l(Kr)[(W+1)\tan\phi_l^{\pm}+(1+l+k^{\pm})/r]}, \tag{2}$$

where $K^2=W^2-1$, j_l, and n_l are, respectively, the regular and the irregular spherical Bessel functions and $\phi_l^{\pm}$ is the limit of $\phi_l^{\pm}(r)$ for $r\to\infty$.

Once the values of the phase shifts are known, the differential elastic scattering cross section can be calculated as[8]

$$\frac{d\sigma}{d\Omega}=|f|^2+|g|^2, \tag{3}$$

where the scattering amplitudes f and g are given by

$$f(\theta)=\frac{1}{2iK}\sum_{l=0}^{\infty}\{(l+1)[\exp(2i\delta_l^{-})-1]+l[\exp(2i\delta_l^{+})-1]\}P_l(\cos\theta), \tag{4}$$

$$g(\theta)=\frac{1}{2iK}\sum_{l=1}^{\infty}[-\exp(2i\delta_l^{-})+\exp(2i\delta_l^{+})]P_l^1(\cos\theta). \tag{5}$$

In these equations P_l represent the Legendre polynomials and

$$P_l^1(x)=(1-x^2)^{1/2}\frac{dP_l(x)}{dx}. \tag{6}$$

The values of $\phi_l^{\pm}$ have been computed by using numerical integration with a fourth-order Runge–Kutta method of the Dirac equation (1). Afterwards they have been used for calculating the phase shifts by using Eq. (2).

 0021-8979/96/79(11)/8406/6/$10.00

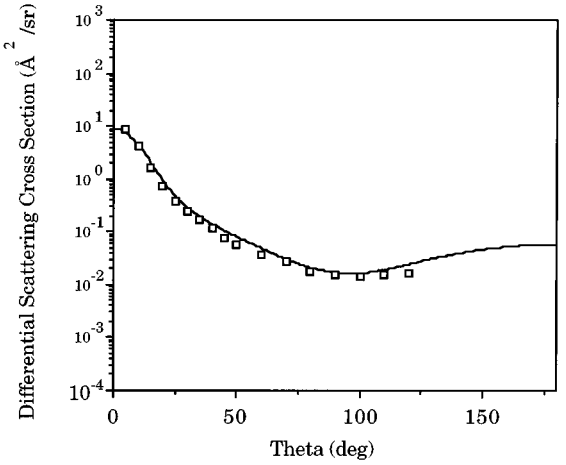

FIG. 1. Comparison of the present theoretical calculation to the experimental data of Iga *et al.* (Ref. 14) concerning the differential elastic scattering cross section of 500 eV electrons in Ar: solid line—theory; squares—experimental data.

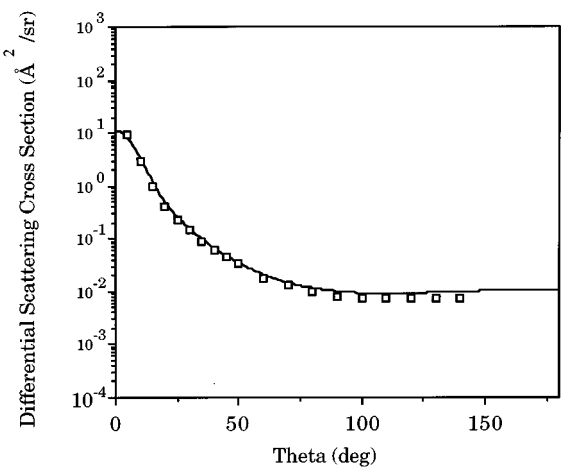

FIG. 2. Comparison of the present theoretical calculation to the experimental data of Iga *et al.* (Ref. 14) concerning the differential elastic scattering cross section of 1000 eV electrons in Ar: solid line—theory; squares—experimental data.

The computation of the total and transport elastic scattering cross sections, respectively defined as

$$\sigma_{\text{tot}} = 2\pi \int_0^{\pi} \frac{d\sigma}{d\Omega} \sin\,\theta d\theta, \tag{7}$$

$$\sigma_{\text{tr}} = 2\pi \int_0^{\pi} (1-\cos\,\theta)\, \frac{d\sigma}{d\Omega} \sin\,\theta d\theta \tag{8}$$

has been performed by applying Bode's rule to the numerically calculated differential cross sections.

III. ELASTIC SCATTERING CALCULATIONS

A. Free atoms

Details about the calculations in the case of interaction with free atoms and comparison with other numerical computations can be found in Refs. 9 and 10. The atomic potential was that of Hartree–Fock for atomic numbers lower than 19 and that of Dirac–Hartree–Fock–Slater for atomic numbers higher than 18. We used the best-fit functions proposed by Cox and Bonham[11] for the Hartree–Fock potential and those proposed by Salvat *et al.*[12] for the Dirac–Hartree–Fock–Slater potential. With respect to the calculations reported in Ref. 9, we have now introduced, in the case of electrons, the exchange effects by adding the Furness and McCarthy expression to the electron atom potential energy:[13]

$$V_{\text{ex}} = \tfrac{1}{2}(E - V_s) - \tfrac{1}{2}[(E-V_s)^2 + 4\pi\rho e^4 a_0]^{1/2}, \tag{9}$$

where E is the electron energy, V_s is the electrostatic scalar potential energy (negative for electron–atom scattering), ρ is the atomic electron density (obtained by the Poisson equation), e is the electron charge and a_0 is the Bohr radius.

Figures 1 and 2 show the comparison of the present theoretical calculations to the experimental data of Iga *et al.*[14] concerning the differential elastic scattering cross section of 500 and 1000 eV electrons in Ar. The comparison to the Holtcamp *et al.* experimental data[15] concerning 300 eV electrons in Hg is shown in Fig. 3.

The introduction of the exchange effects improves the accuracy of the calculation for the low angle differential elastic scattering cross section at low energies and, as a consequence, the computation of the total elastic scattering cross section: In Tables I and II the experimental electron atom total scattering cross sections, as reported by Jansen *et al.*,[16] DuBois and Rudd,[17] Iga *et al.*[14] and Holtkamp *et al.*,[15] are compared to the theoretical computation.

B. Atoms bound in solids

Solid-state effects should be introduced when the target atom is bound in a solid. Here we will introduce solid-state

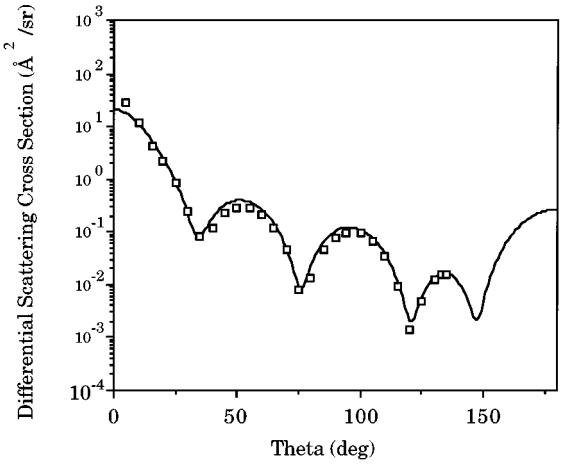

FIG. 3. Comparison of the present theoretical calculation to the Holtcamp *et al.* experimental data (Ref. 15) concerning 300 eV electrons in Hg: solid line—theory; squares—experimental data.

TABLE I. Total elastic scattering cross section in units of Å^2 of electrons impinging on Ar atoms.

E_0 (eV)	Jansen *et al.* (1976)	DuBois and Rudd (1976)	Iga *et al.* (1987)	Present work
50	⋯	7.17	⋯	7.38
100	3.81	4.79	⋯	4.32
200	3.02	3.05	⋯	3.05
400	⋯	⋯	2.13	2.20
500	1.99	2.02	1.71	1.97
800	⋯	1.35	1.31	1.52
1000	⋯	⋯	1.35	1.34

effects and give tabulations of the total and transport cross section for medium energy (500–4000 eV) electrons and positrons in solid Al, Cu, Ag, and Au.

When the target atom is bound in a solid the outer orbitals of the atom are modified. In order to consider such alterations, solid-state effects have been introduced by using the muffin–tin model in which the potential of each atom of the solids is altered by the nearest neighbor. The radius of the Wigner–Seitz sphere is as follows:

$$r_{\mathrm{WS}}=0.7346(A/\delta)^{1/3}\ \text{Å}, \tag{10}$$

where A is the atomic weight and δ is the mass density (q/cm^3). Assuming that the nearest neighbor is located at a distance of $2r_{\mathrm{WS}}$, the resulting potential, for $r<r_{\mathrm{WS}}$, is given by

$$V_{\mathrm{solid}}(r)=V(r)+V(2r_{\mathrm{WS}}-r)-2V(r_{\mathrm{WS}}) \tag{11}$$

and is the equal of zero elsewhere.

The term $2V(r_{\mathrm{WS}})$, introduced in order to shift the energy scale so that $V_{\mathrm{solid}}(r\geqslant r_{\mathrm{WS}})=0$, has also been subtracted from the kinetic energy of the incident particle. This approach for describing elastic scattering in solids has been adopted, for example, by Salvat and Mayol.[18]

In Figs. 4 and 5 the differential elastic scattering cross section for, respectively, 1 keV electrons and 1 keV positrons in gold are presented. Similar results have recently been reported by Czyzewski *et al.*[19] and Kawata and Ohya.[20] The total and the transport elastic scattering cross sections for electrons and positrons in Al, Cu, Ag, and Au are reported in Tables III–VI.

The comparison of the present tabulation with the data reported in Ref. 9 confirms that the solid-state and the exchange effects have little influence on the transport elastic

TABLE II. Total elastic scattering cross section in units of Å^2 of electrons impinging on Hg atoms.

E_0 (eV)	Holtkamp *et al.* (1987)	Present work
100	8.99	8.64
150	7.95	7.24
300	4.93	4.72

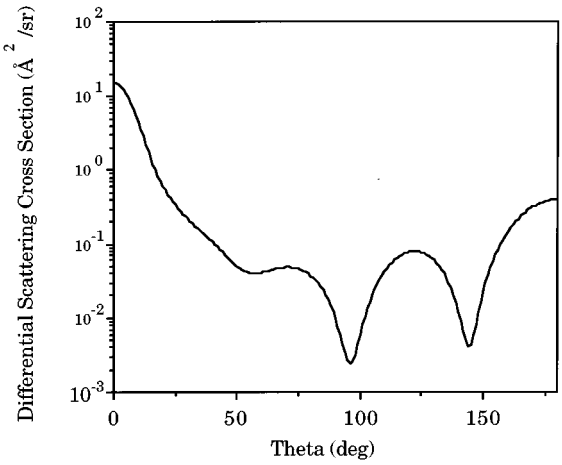

FIG. 4. Theoretical differential elastic scattering cross section for 1000 eV electrons in gold.

scattering cross section. The total elastic scattering cross section, on the other hand, is strongly influenced by the solid state and the exchange.

IV. RESULTS AND DISCUSSION

A. The mean number of wide-angle collisions and the backscattering coefficient

It has been shown in recent papers[21,22] that the reflection coefficient is a function of the mean number of wide-angle collisions. If R is the range of penetration defined by

$$R=\int_{E_0}^{0}\frac{dE}{dE/ds}, \tag{12}$$

where dE/ds is the energy lost per unit of length and E_0 is the primary energy, then the mean number of wide-angle collisions is defined as

$$\nu=NR\sigma_{\mathrm{tr}}, \tag{13}$$

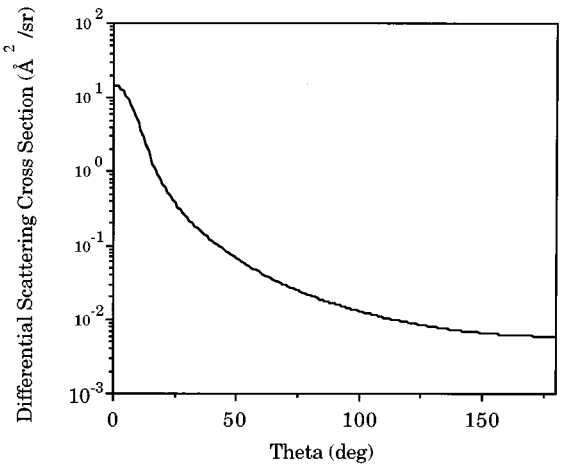

FIG. 5. Theoretical differential elastic scattering cross section for 1000 eV positrons in gold.

TABLE III. Total elastic scattering cross section in units of Å^2 of electrons impinging on atoms bound in solids.

E_0 (eV)	Al	Cu	Ag	Au
500	1.43	1.58	2.46	2.86
1000	0.919	1.12	1.82	2.09
1500	0.694	0.914	1.52	1.77
2000	0.563	0.784	1.33	1.57
2500	0.476	0.694	1.19	1.42
3000	0.412	0.625	1.09	1.31
3500	0.365	0.572	1.01	1.22
4000	0.327	0.528	0.940	1.15

TABLE IV. Total elastic scattering cross section in units of Å^2 of positrons impinging on atoms bound in solids.

E_0 (eV)	Al	Cu	Ag	Au
500	1.24	1.25	2.03	2.33
1000	0.808	0.937	1.58	1.84
1500	0.618	0.779	1.34	1.58
2000	0.506	0.678	1.19	1.42
2500	0.431	0.606	1.08	1.30
3000	0.376	0.551	0.988	1.20
3500	0.335	0.507	0.918	1.12
4000	0.302	0.470	0.860	1.06

TABLE V. Transport elastic scattering cross section in units of Å^2 of electrons impinging on atoms bound in solids.

E_0 (eV)	Al	Cu	Ag	Au
500	0.306	0.706	1.04	1.01
1000	0.115	0.319	0.522	0.709
1500	0.0623	0.187	0.321	0.489
2000	0.0397	0.126	0.222	0.359
2500	0.0278	0.0912	0.165	0.278
3000	0.0206	0.0698	0.128	0.223
3500	0.0160	0.0554	0.104	0.183
4000	0.0128	0.0453	0.0857	0.155

TABLE VI. Transport elastic scattering cross section in units of Å^2 of positrons impinging on atoms bound in solids.

E_0 (eV)	Al	Cu	Ag	Au
500	0.132	0.220	0.338	0.405
1000	0.0612	0.119	0.187	0.238
1500	0.0371	0.0796	0.127	0.170
2000	0.0254	0.0587	0.0943	0.131
2500	0.0187	0.0457	0.0742	0.106
3000	0.0144	0.0370	0.0605	0.0889
3500	0.0115	0.0307	0.0507	0.0761
4000	0.00945	0.0260	0.0433	0.0663

TABLE VII. Mean number of wide-angle collisions suffered by the electrons before slowing down to rest.

E_0 (eV)	Al	Cu	Ag	Au
500	2.73	4.71	3.65	3.10
1000	2.70	4.99	4.58	5.35
1500	2.60	4.96	4.94	6.38
2000	2.53	4.96	5.13	6.95
2500	2.49	4.92	5.27	7.38
3000	2.44	4.92	5.34	7.68
3500	2.42	4.91	5.46	7.88
4000	2.40	4.91	5.50	8.12

where N is the number of atoms per unit of volume in the solid target. Actually, due to the energy loss of the particles inside the solid targets, Eq. (13) only gives an approximate evaluation of the mean number of wide-angle collisions. Anyway, $Nr\delta_{\mathrm{tr}}$ is the quantity we need in order to compute the backscattering coefficient.

The computation of the range was performed by Gaussian quadrature of the polynomial best fits of the stopping power numerical results given by Ashley.[23] The integration was performed from the primary energy E_0 to 100 eV instead of 0 eV. The residual range was neglected because very low energy electrons generally are not included in the experimental evaluation of the backscattering coefficient.

Tables VII and VIII give the values of ν as a function of the primary energy for medium energy electrons and positrons. Since ν is smaller for the positrons than for the electrons it is concluded that the electrons have a larger probability of backscattering than the positrons.

The values of the backscattering coefficient η obtained by using the Vicanek and Urbassek theory,[22] expressed, for normal incidence, by

$$\eta=\left(1+a_1\frac{1}{\nu^{1/2}}+a_2\frac{1}{\nu}+a_3\frac{1}{\nu^{3/2}}+a_4\frac{1}{\nu^2}\right)^{-1/2} \tag{14}$$

are reported in Tables IX and X [the values of the coefficients a_i $(i=1,2,3,4)$ can be found in Ref. 22].

The presented data are in agreement with recent experimental and Monte Carlo results.[24–28]

TABLE VIII. Mean number of wide-angle collisions suffered by the positrons before slowing down to rest.

E_0 (eV)	Al	Cu	Ag	Au
500	0.84	1.06	0.85	0.93
1000	1.06	1.40	1.26	1.40
1500	1.17	1.63	1.53	1.78
2000	1.25	1.83	1.74	2.06
2500	1.30	1.98	1.91	2.31
3000	1.35	2.11	2.05	2.53
3500	1.38	2.22	2.18	2.72
4000	1.42	2.31	2.28	2.89

TABLE IX. Electron backscattering coefficients.

E_0 (eV)	Al	Cu	Ag	Au
500	0.198	0.303	0.251	0.220
1000	0.197	0.315	0.297	0.331
1500	0.191	0.314	0.313	0.370
2000	0.187	0.314	0.321	0.390
2500	0.184	0.312	0.327	0.404
3000	0.181	0.312	0.330	0.414
3500	0.180	0.311	0.335	0.420
4000	0.178	0.312	0.337	0.427

B. Comparisons with other calculations

Backscattering coefficients of positrons and electrons have been reported by various authors.

With respect to fast electrons, a much experimental data have been reported and analytical and Monte Carlo models have been proposed which are rather satisfactory (see, e.g., Refs. 29–31).

The case of low energy is more difficult because the first Born approximation for elastic scattering is not valid and a screened Rutherford formula cannot be used. Concerning the inelastic events, the Bethe formula is not usable for low energies.

As demonstrated in Ref. 22 the analytical calculation of the backscattering coefficients for light ions can be performed by using tabulations of the mean number of wide-angle collisions. Here tabulations of such a quantity for low energy electrons and positrons are provided. It is a goal of this article to demonstrate that the backscattering coefficients computed by using these tabulations are in better agreement with available experimental data than earlier works concerning the modeling of slow electrons and positrons reflected from solid targets.

Tables XI and XII compare the results of recently reported valuable Monte Carlo simulations with the Coleman *et al.* experimental data:[25] A comparison with the values reported in Table X clearly demonstrates that the present computation is in better agreement with experiment than previous calculations.

C. Discussion

Backscattering coefficient calculation requires a very accurate knowledge of elastic scattering processes. In Sec. IV B an improvement with respect to previous calculations was shown. Possible reasons for the improvement are discussed here.

The proposed tabulations of total and transport elastic scattering cross section have been obtained by using the recent and very accurate descriptions of the atomic potential given by Salvat *et al.*[12] The results, as shown by comparison of elastic scattering cross section with experimental data, are very good. The reasons for this are as follows: the Dirac equation was used instead of the Schrödinger equation for the phase shifts computation; a very accurate atomic potential was used; and for the electrons, the atomic potential was modified by using a realistic exchange potential.[13] Furthermore the calculations of the mean number of wide-angle collisions in a solid target suffered by the particle before slowing down to rest, a quantity related to the backscattering coefficient,[22] were performed after the introduction of solid-state effects in the atomic potential.

Another point to note is the use of the theory of Vicanek and Urbassek[22] instead of Monte Carlo simulation. Simulations involve approximations due to the interpolations of the differential elastic scattering cross section at each step of the particle trajectory.

Indeed, in order to obtain statistically significant results, the number of trajectories in a typical Monte Carlo simulation must be about 10^4–10^5. At each step of the trajectories the particle kinetic energy is different and elastic scattering cross section should be recalculated. Since the calculation of differential elastic cross section for low energy electrons and positrons is rather time consuming, Monte Carlo simulations

TABLE X. Positron backscattering coefficients.

E_0 (eV)	Al	Cu	Ag	Au
500	0.069	0.085	0.069	0.076
1000	0.086	0.110	0.100	0.111
1500	0.094	0.127	0.120	0.137
2000	0.099	0.140	0.134	0.156
2500	0.104	0.151	0.146	0.172
3000	0.107	0.159	0.156	0.186
3500	0.109	0.166	0.164	0.198
4000	0.112	0.172	0.171	0.208

TABLE XI. Backscattering coefficients of 1 keV positrons: present calculation compared to experimental data and to other calculations. Aers's data: Best fit of Aers's Monte Carlo data.

Z	Coleman *et al.* Experimental data (1992)	Coleman *et al.* Monte Carlo data (1992)	Aers Monte Carlo data (1994)	Ghosh and Aers Monte Carlo data (1995)	Present
13	0.069	0.109	0.104	0.118	0.086
29	0.135	0.156	0.152	0.122	0.110
47	0.106	0.126	0.130	0.186	0.100
79	0.123	0.168	0.165	0.179	0.111

TABLE XII. Backscattering coefficients of 3 keV positrons: present calculation compared to experimental data and to other calculations. Aers's data: Best fit of Aers's Monte Carlo data.

Z	Coleman *et al.* Experimental data (1992)	Coleman *et al.* Monte Carlo data (1992)	Aers Monte Carlo data (1994)	Ghosh and Aers Monte Carlo data (1995)	Present
13	0.086	0.115	0.115	0.123	0.107
29	0.177	0.194	0.188	0.138	0.159
47	0.168	0.182	0.175	0.227	0.156
79	0.186	0.242	0.232	0.239	0.186

generally use interpolations from available tabulations instead of direct computation.

In conclusion, the use of the analytical expression of Vicanek and Urbassek and the transport cross section instead of the interpolation of the differential cross section make the calculation of the low energy backscattering coefficients both less time consuming and in better agreement with experiment. This is very useful, especially when backscattering coefficient knowledge is necessary for the calculation of the backscattering of electrons from thin films[32] and multilayers,[33] for the depth distribution computation of thermalized positrons,[34] and so on.

V. CONCLUSION

The calculation of low–medium energy electrons and positrons transport in solid targets requires an accurate knowledge of the elastic scattering cross section. In this article tabulations of the total and transport elastic scattering cross sections for electrons and positrons in solid targets have been given. Exchange (for electron scattering) and solid-state effects were included because they influence the differential and total scattering cross sections.

By using the calculated data the possibility of obtaining rather accurate results concerning backscattering of slow electrons and positrons impinging on solid targets has been shown.

ACKNOWLEDGMENTS

The author wishes to thank Professor Antonio Miotello (University of Trento) and Dr. Fabio Marchetti (ITC, Trento) for their helpful and stimulating comments. The author is also indebted to Nadia Oss Papot (IRST, Trento) for her skillful technical assistance.

[1] H. Niedrig, J. Appl. Phys. **53**, R15 (1982).
[2] G. Messina, A. Paoletti, S. Santangelo, and A. Tucciarone, La Rivista del Nuovo Cimento **15**, 1 (1992).
[3] A. Dupasquier and A. Zecca, La Rivista del Nuovo Cimento **8**, 1 (1985).
[4] P. J. Schultz and K. J. Lynn, Rev. Mod. Phys. **60**, 701 (1988).
[5] P. Asoka-Kumar, K. G. Lynn, and D. O. Welch, J. Appl. Phys. **76**, 4935 (1994).
[6] S. R. Lin, N. Sherman, and J. K. Percus, Nucl. Phys. **45**, 492 (1963).
[7] P. J. Bunyan and J. L. Schonfelder, Proc. Phys. Soc. **85**, 455 (1965).
[8] N. F. Mott, Proc. R. Soc. London Ser. A **124**, 425 (1929).
[9] M. Dapor, Nucl. Instrum. Methods B **95**, 470 (1995); **108**, 363 (1996).
[10] M. Dapor, J. Appl. Phys. **77**, 2840 (1995).
[11] H. L. Cox, Jr. and R. A. Bonham, J. Chem. Phys. **47**, 2599 (1967).
[12] F. Salvat, J. Martínez, R. Mayol, and J. Parellada, Phys. Rev. A **36**, 467 (1987).
[13] J. B. Furness and I. E. McCarthy, J. Phys. B **6**, 2280 (1973).
[14] I. Iga, L. Mu-Tao, J. C. Nogueira, and R. S. Barbieri, J. Phys. B Atom. Mol. Phys. **20**, 1095 (1987).
[15] G. Holtcamp, K. Jost, F. J. Peitzmann, and J. Kessler, J. Phys. B Atom. Mol. Phys. **20**, 4543 (1987).
[16] R. H. J. Jansen, F. J. de Heer, H. J. Luyken, B. van Wingerden, and H. J. Blaauw, J. Phys. B Atom. Mol. Phys. **9**, 185 (1976).
[17] R. D. DuBois and M. E. Rudd, J. Phys. B Atom. Mol. Phys. **9**, 2657 (1976).
[18] F. Salvat and R. Mayol, Comput. Phys. Commun. **74**, 358 (1993).
[19] Z. Czyzewski, D. O'Neil MacCallum, A. Romig, and D. C. Joy, J. Appl. Phys. **68**, 3066 (1990).
[20] J. Kawata and K. Ohya, Nucl. Instrum. Methods B **90**, 29 (1994).
[21] J. V. Vukanic, R. K. Janev, and D. Heifetz, Nucl. Instrum. Methods B **18**, 131 (1987).
[22] M. Vicanek and H. M. Urbassek, Phys. Rev. B **44**, 7234 (1991).
[23] J. C. Ashley, J. Electron. Spectrosc. Relat. Phenom. **50**, 323 (1990).
[24] G. R. Massoumi, N. Hozhabri, W. N. Lennard, and P. J. Schultz, Phys. Rev. B **44**, 3486 (1991).
[25] P. G. Coleman, L. Albrecht, K. O. Jensen, and A. B. Walker, J. Phys. Condens. Matter **4**, 10 311 (1992).
[26] J. Mäkinen, S. Palko, J. Martikainen, and P Hautojärvi, J. Phys. Condens. Matter **4**, L503 (1992).
[27] G. C. Aers, J. Appl. Phys. **76**, 1622 (1994).
[28] V. J. Ghosh and G. C. Aers, Phys. Rev. B **51**, 45 (1995).
[29] T. E. Everhart, J. Appl. Phys. **31**, 1483 (1960).
[30] G. D. Archard, J. Appl. Phys. **32**, 1505 (1961).
[31] M. Dapor, Phys. Rev. B **46**, 618 (1992).
[32] M. Dapor, Phys. Rev. B **43**, 10118 (1991); **44**, 9784 (1991).
[33] M. Dapor, Phys. Rev. B **48**, 3003 (1993).
[34] M. Dapor, Scanning Microsc. **9**, 939 (1995).